

Production of Metastable Mercury Atoms by Electron Impact*

Walter L. Borst[†]

Department of Physics, University of California, Berkeley, California 94720

(Received 8 August 1968; revised manuscript received 12 November 1968)

Excitation of Hg atoms by electron impact, particularly into metastable states, was studied in the energy range 4 to 15 eV. The excitation function for the 6^3P_2 metastable state (5.46 eV) was measured from threshold up to 8.5 eV. The absolute cross-sectional scale for this state was calibrated by monitoring slow inelastically scattered electrons near threshold. The cross section had a maximum value of $3.2 \times 10^{-16} \text{ cm}^2 \pm 25\%$ (rms) at 5.75 eV and dropped to half this value at about 8 eV. An electron beam of 0.1-eV half-width was produced by the Retarding Potential Difference RPD method. Excited atoms were detected by electron ejection from a tungsten surface. The secondary electron yield for the 6^3P_2 state was typically 2×10^{-4} . Pronounced structure in the detector current with maxima at 9.00 and 9.60 eV was attributed to the 7^3P_1 state (8.64 eV). It appears that the contribution of the $6p' \ ^3D_3^0$ metastable state was minor. An upper limit of a few times 10^{-18} cm^2 was estimated for the maximum cross section of this state. Another region of structure in the total detector current occurred close to and above ionization threshold. Experimental evidence indicates that this structure was produced by long-lived auto-ionizing states.

I. INTRODUCTION

Few measurements exist on metastable excitation functions for the electron-impact excitation of Hg.^{1,2} No measurements of absolute metastable excitation cross sections have been reported. On the other hand, optical excitation functions and cross sections have been measured quite extensively,³⁻⁵ recently with very good energy resolution,⁶ which unmasked sharp structure. Since Hg is of considerable interest in gaseous electronics, it was attempted to study the excitation of this atom into metastable states with good energy resolution.

The direct starting point for the present investigation came from an investigation by Rostron⁷ in which fast (around kiloelectron volts) excited Hg atoms were produced by charge exchange of Hg^+ ions in Hg vapor. As a result the following very interesting features were observed: (1) There was a large secondary electron emission produced at a tungsten target by either fast or excited neutrals with yields as high as 0.4. (2) The appearance of what were observed to be stable or at least long-lived, negative ions of Hg. (3) An unexpected lifetime for some of the assumed excited states, presumably metastable, with groups of particles having lifetimes of the order of 10^{-5} sec. The repetition of Rostron's experiment by the present author under improved conditions indicated, first, that there were indeed large target currents due to these fast neutrals. Second, there was no clear evidence of the existence of negative ions. Negative currents appeared in the target chamber. These were then ascribed to the probable emission of positive ions from the target by surface ionization of excited states. This inter-

pretation followed from Varney's⁸ discovery in argon of surface ionization of excited atoms at a metal target.

In view of the widespread scattering of the fast neutrals on electrodes of the target assembly and to eliminate kinetic-energy effects at the target, it was felt that this type of study was not adequate, accordingly measurements were undertaken with slower particles of known excitation energies. This was achieved by using the electron-impact excitation of thermal Hg atoms at known energies. With these, careful analysis of the appearance of secondary emission from the target produced by metastables and photons was carried out as a function of electron beam energy, using the Retarding Potential Difference (RPD) method combined with a trapped-electron method. Care was taken to avoid space charge effects, to ascertain the source and nature of the observed target current, and to calibrate the energy scale to 0.1 eV over the whole energy range. Having achieved this, various phenomena were observed. These indicated: (1) That the lowest energy metastables capable of liberating electrons from the partly contaminated W target were those in the 6^3P_2 state and neither the two resonance states nor the 6^3P_0 metastable state were responsible. (2) It was proven that the second group of emission was caused by photons from the 7^3P_1 state (8.64 eV). Very little, if any, contribution of the $^3D_3^0$ metastable state (9.06 eV) as reported by Lichten,⁹ could be clearly delineated. (3) Finally, a large target current was observed near ionization threshold. It is very likely that this current is to be associated with the excited states observed by Rostron. Moreover, in this region the presence of positive ions in the collection space was as-

certained. There were no direct means available for ascertaining whether these positive ions came from surface ionization of excited atoms or from auto-ionization of long-lived excited particles.

II. APPARATUS

The experimental arrangement consisted basically of an electron gun, a collision chamber CC, a metastable atom detector T, and detectors T_1 , T_2 for slow inelastically scattered electrons [Fig. 1(A)].

The electron gun was operated in the RPD mode, which has been described in detail.¹⁰ The electron-beam difference current was about 4×10^{-8} A with a half-width of 0.1 eV. The electron beam was collimated by an axial magnetic field of about 100 G.

Metastable atoms produced in CC were able to reach the cylindrical tungsten detector T, where they ejected secondary electrons, provided their excitation energy was greater than the work function of T.¹¹ Secondary electrons were collected by the positively biased end plates T_1 and T_2 , and grid G_2 . The total metastable excitation function was obtained by monitoring the secondary electron current leaving T as a function of electron energy. In order to distinguish between photoelectrons and secondary electrons, the detector in a duplicate tube was divided into two parts T_p and T_m [Fig. 1(B)]. A quartz tubing installed in the space between G_2 and G_3 allowed only photons (with wavelength longer than 1700 Å) to reach T_p , whereas both metastable atoms and photons could reach T_m .

In typical operation, the grids G_1 , G_3 , the shields, detector T, and electron collector C were kept at ground potential. A positive potential of +18 V was applied to G_2 , T_1 , and T_2 .

The penetration of the positive potential on G_2 onto the axis of CC was about +0.1 V. Inelastically scattered electrons with energies smaller than 0.1 eV could not pass the end plates of CC and were thus trapped in CC. These electrons could leave CC only by diffusion through G_1 against the axial magnetic field. Essentially all trapped electrons were collected at T_1 , T_2 because of potential penetration from T_1 , T_2 into the space between G_1 and G_3 . In distinction to the trapped-electron method introduced by Schulz,¹² slow inelastically scattered electrons are collected axially in the present case. Thereby the function of the end plates T_1 , T_2 is twofold. Besides collecting trapped electrons, T_1 , T_2 also collected secondary electrons ejected from the metastable detector T. The axial magnetic field prevented most secondary electrons from reaching G_2 .

Secondary electron currents were several orders of magnitude smaller than trapped electron currents. Thus excitation functions and trapped electrons could be monitored simultaneously.

The positive potential on T_1 and T_2 resulted in a higher sensitivity for measuring excitation functions. The secondary electron current leaving T increased by about a factor of 3 and saturated if T_1 , T_2 were made a few volts positive. Under this condition essentially all secondary electrons left T. This was verified for He, where the cross section for the production of the 2^3S_1 metastable state^{13,14} and the secondary yield are known.¹⁵

Neither positive ions nor electrons from CC were able to reach T. Positive ions were repelled by G_2 , T_1 , and T_2 . Electrons from CC were collected at T_1 and T_2 .

Ultrahigh vacuum techniques employing a mercury diffusion pump, liquid-nitrogen cooled traps, and bakeable valves were used. The background pressure in the tube was about 1×10^{-9} Torr. The pressure calibration of an ionization gauge was achieved by using the known vapor-pressure curve in the case of Hg. For He, the ionization gauge was calibrated against a McLeod gauge. The error in absolute pressure measurement was 10% or less.

It was verified that target as well as trapped electron currents were proportional to the gas pressure in the tube. Therefore the measured currents were solely due to single exciting col-

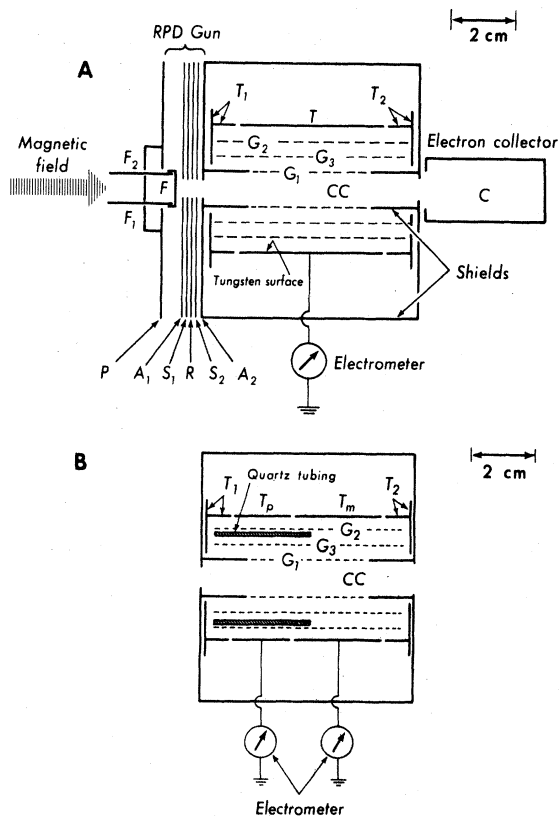
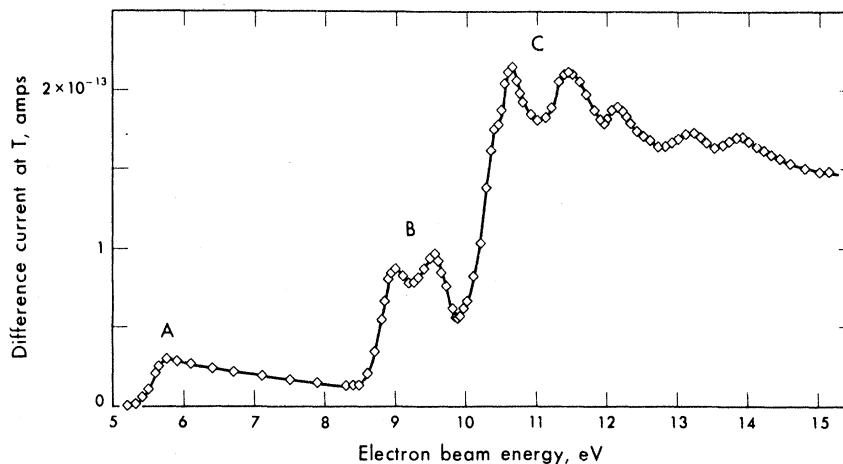


FIG. 1. (A) Schematic of experimental tube. (B) Altered tube to distinguish between secondary electrons and photoelectrons.

FIG. 2. Detector current as a function of electron-beam energy. (The term "difference current" refers to the use of the RPD method.) Structure *A* represents the excitation function of the 6^3P_2 metastable state up to 8.5 eV. Structure *B* is mainly produced by photoelectrons from the 7^3P_1 state. Structure *C* with peaks at 10.65, 11.45, 12.15, 13.20, and 13.85 eV is due to positive ions from long-lived auto-ionizing states and to a smaller extent to secondary electrons.



lisions between beam electrons and unexcited gas atoms.

III. RESULTS

A. Detector Current

The detector current as a function of energy is shown in Fig. 2. Pronounced structure occurs around three regions of energy *A*, *B*, and *C*, of which the significance is discussed below.

In order to ascertain the proper functioning of the apparatus, the total metastable excitation of He was measured. Complete agreement was found with the curve obtained by Schulz and Fox.¹⁴

B. Trapped Electrons

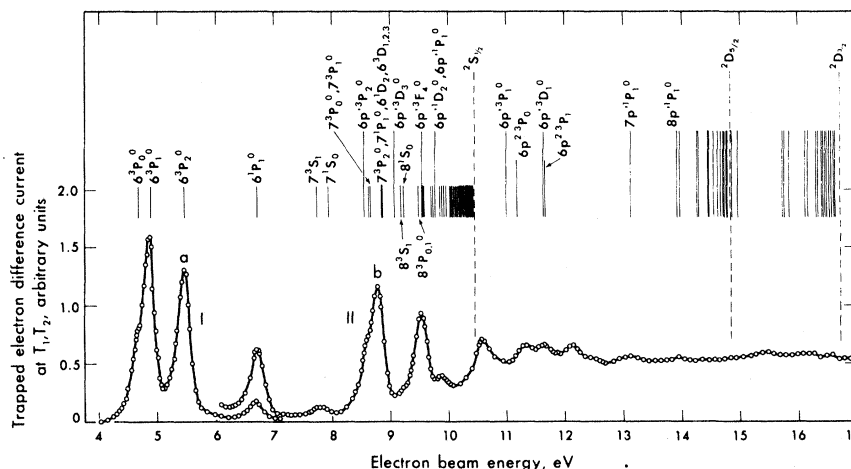
The trapped electron current as a function of energy is shown in Fig. 3. Schulz¹² first monitored trapped electrons in Hg up to ionization threshold. The gross features of both measurements below ionization threshold are the same. However the ratios of peak heights differ, probably because somewhat different well depths were used. In the present case, it was found that the ratio of peak heights in Fig. 3 depended on the

well depth. This is to be expected if the excitation function has sharp structure within an energy range above threshold given by the well depth. In particular this is true for the 6^3P_1 resonant state. This complication is not present for the 6^3P_2 metastable state and the cross section can be easily obtained from the height of the 6^3P_2 peak in Fig. 3. Above ionization threshold, the structure in Fig. 3 appears to be related to structure in the total detector current (Fig. 2). The magnitude of the trapped electron current is probably distorted in this energy domain because of space charge neutralization by Hg^+ ions. However, the energy scale is undistorted and so is the position of structure.

C. Energy Scale and Space Charge Effects

The absolute energy scale was calibrated by means of beam retardation, trapped electrons, and the onsets of Hg^+ ions and He metastable atoms.¹⁶ Hg^+ ions were monitored at grid G_3 [Fig. 1(A)] which in this case was at -2V. The ionization function thus obtained is shown in Fig. 4 and compared with measurements of Hickam¹⁷ and Nottingham.¹⁸ The four methods of calibration

FIG. 3. Trapped electron current as a function of electron-beam energy. Curve II was taken with a 3.5 times higher sensitivity than curve I. Both curves are slightly shifted in energy such that the 6^1P_1 peak coincides with the 6^1P_1 level. Above ionization threshold the magnitude of the current may be distorted. However, the position of structure is undistorted.



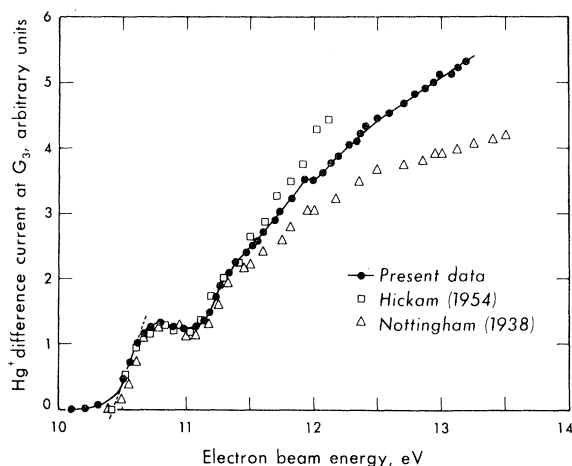


FIG. 4. Ionization probability curve of Hg near threshold. The three sets of data are normalized in magnitude at the peak.

covering the energy range from 0 to 20 eV yielded the same energy scale within 0.1 eV or better.

From this it follows that any space charge potentials were smaller than 0.1 V within this energy range. For beam electrons and positive ions, maximum space charge potentials of 0.01 and 0.04 V, respectively, were calculated. This is consistent with the experimental values.

The *calculated* space charge potential due to trapped electrons was too large by more than an order of magnitude.¹⁶ For this calculation use was made of the radial diffusion time for trapped electrons in the presence of a magnetic field with an assumed zero electric field.¹² Clearly, trapped electrons can only produce a space charge potential smaller in magnitude than the well depth along the axis of CC. Otherwise, slow electrons would be no longer trapped. The actual space charge potential was much smaller than the well depth because the peaks in Fig. 3 are properly spaced. Further, the ratio of peak heights for the 6^3P_2 and 6^1P_1 states did not depend on beam current despite the quite different peak heights for these states.

It is believed that potential gradients in CC, particularly near grid G_1 [Fig. 1(A)] shortened the diffusion time, thus reducing the space charge potential to a negligible value.

IV. FURTHER RESULTS AND DISCUSSION

A. The 6^3P_2 Metastable State

Structure A in Fig. 2 represents the excitation function of the 6^3P_2 metastable state (5.46 eV) up to 8.5 eV. Figure 5 shows this curve taken with higher sensitivity, and a comparison with other data. The initial rise of the excitation function appears to be linear. The threshold energy ob-

tained by linear extrapolation is (5.45 ± 0.10) eV and agrees well with the 6^3P_2 level. There was no detectable photoelectron contribution from the 6^3P_1 and 6^1P_1 resonant states (see level diagram, Fig. 6). This is evident in Fig. 2 and Fig. 5 and was also verified with the quartz window [Fig. 1(B)] in a later measurement.

The absolute cross section was determined from the trapped electron current at the 6^3P_2 peak in Fig. 3. The peak current for an individual state is given by

$$I = I_b n Q(\Delta E) l_t, \quad (1)$$

where I_b is the beam current, n the gas density, $Q(\Delta E)$ the cross section at an energy ΔE above threshold, l_t the effective length of the collision chamber for the production of trapped electrons. The energy ΔE is equal in magnitude to the penetrating potential from grid G_2 [Fig. 1(A)]. In Eq. (1) a collection efficiency of 100% for trapped electrons at the endplates T_1 and T_2 was assumed, because all trapped electrons had to diffuse through grid G_1 and only a negligible number of them reached the grids G_3 and G_2 .

If a linear threshold law is assumed, Eq. (1) becomes

$$I = I_b n (dQ/dE) \Delta E l_t, \quad (2)$$

where $dQ/dE = \text{const}$ near threshold. The effective length l_t was taken as the length of grid G_1 .¹⁶ The slope dQ/dE for the 6^3P_2 state was obtained from (2), as all the other quantities were known. The result is

$$(dQ/dE)(6^3P_2) = 1.1 \times 10^{-15} \text{ cm}^2/\text{eV}. \quad (3)$$

The rms and maximum errors to be assigned to this value are 25 and 40%, respectively. The error is due to uncertainties in ΔE , l_t , and n , and

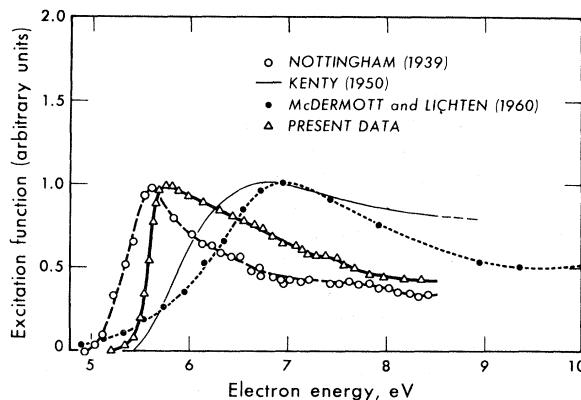


FIG. 5. Excitation functions for the 6^3P_2 metastable state. The curves are normalized to the same maximum height.

B. Energy Region 8.5 to 10.0 eV

The pronounced structure *B* in Fig. 2 has a threshold energy of (8.65 ± 0.10) eV. This agrees only with the radiative 7^3P_1 (8.64 eV) level (Fig. 6). The 7^3P_0 state can be excluded. It does not radiate directly to the ground state and any cascading transitions in the optical region including the two resonance lines produce no detectable amount of photoelectrons. Cascading to the 6^3P_2 metastable state does not play a significant role.¹⁶ The 7^3P_1 state being a mixed state can radiate directly to the ground state. The resulting photons have enough energy to eject electrons from the detector with a high yield. The yield was of the order of 0.01. This agrees with measurements of the established general photoelectric response for tungsten,^{21, 22} which shows a sharp increase in yield above 8 eV. Although photons with energies greater than 7.6 eV (1700 Å) were not transmitted by the quartz window [Fig. 1(B)], it was established on the basis of threshold energy that structure *B* up to 9.0 eV was caused by the 7^3P_1 state. Even above 9.0 eV the 7^3P_1 dominates and structure *B* represents part of the excitation function for this state since it could be shown that cascading transitions to the 7^3P_1 state do not contribute to structure *B*.¹⁶ Comparison with the excitation function for the 6^3P_1 resonant state, which also exhibits two major peaks,⁶ is interesting. There, the first peak can be associated with a resonance.^{23, 24} For the second prominent peak, no corresponding resonance has been found.²³ A similar situation may apply in the case of the 7^3P_1 state. The position of the peak at 9.00 eV in Fig. 2 agrees with a pronounced resonance at 8.99 eV,²³ whereas the second peak at 9.60 eV does not correspond to a known resonance. Originally it was assumed that structure *B* was caused by the $3D_3^0$ state (9.06 eV), which Lichten⁹ found to be metastable. It is not clear what the shape of the excitation function for this state is, as the two existing excitation functions do not agree.^{1, 9} In the present case, the $3D_3^0$ metastable state must have played a minor role. This can be seen from the trapped-electron data. In Fig. 3 the 7^3P_1 (and 7^3P_0) state did produce structure, whereas a deep minimum occurred at the $3D_3^0$ level. The cross section for the channel $7^3P_1 - 6^1S_0$ was estimated to be 1×10^{-17} cm² at 9.00 eV with a possible error of a factor of 2.¹⁶ In distinction to this, the maximum cross section for the $3D_3^0$ metastable state must be smaller than a few times 10^{-18} cm².

C. Energy Region Above 10.0 eV

The third distinct region of structure occurs at energies close to and above ionization threshold. There are many long-lived levels just below ionization threshold which can produce secondary electrons. Above ionization threshold, auto-ionization appears to be the dominant process. It is

to be noted that only ions from the space between grid G_2 and detector T and not from any other region [Fig. 1 (A)] can reach T. Therefore the auto-ionizing states must be long lived.

Various checks were performed to ascertain the presence of positive ions and electrons from auto-ionizing atoms in the space between G_2 and T.¹⁶ One of these checks consisted in reversing the potential on G_2 from the usual +18 to -18 V. It was observed that the detector current remained zero up to the ionization threshold and then became negative, thereby showing a similar energy dependence as the structure *C* in Fig. 2. This negative current was ascribed to electrons from auto-ionizing states. In another check the spacing between G_2 and T was reduced. This resulted in a smaller height of structure *C*, thus indicating a lifetime of the auto-ionizing states of the order of 10^{-5} to 10^{-4} sec.

Originally it was assumed that the negative current observed under the conditions above was due to positive surface ionization of metastable atoms at the detector, in analogy to the observations of Varney⁸ in argon. Analysis of the data appeared to indicate that auto-ionization was dominant in this arrangement. However, a small contribution from surface ionization cannot be excluded. The peaks in Fig. 2 above ionization threshold do not correspond to known levels of Hg. A comparison between Fig. 2 and Fig. 3 shows, that structure in detector and trapped electron current are related. The energy levels inserted in Fig. 3 above ionization threshold are not associated with the structure observed in Fig. 2, because they were reached by absorption spectroscopy²⁵ and thus represent short-lived states. Hickam¹⁷ postulated the existence of unknown optically forbidden states in order to account for details in the ionization probability curve. Although structure *C* does not represent an ionization probability curve, some of its details may contribute to this curve. This applies in particular to the first peak of structure *C* which may be related to the peak in the ionization probability curve (Fig. 4).

The presence of auto-ionization of long-lived states also casts some light on the existence of the apparent stable, or at least long-lived, Hg^- ion as observed by Rostron⁷ in a charge-exchanged Hg beam. It appears likely from the present work that some of these excited neutrals were producing electrons by auto-ionization. These electrons would account for the negative charges which Rostron ascribed to the presence of Hg^- ions.

ACKNOWLEDGMENTS

I wish to thank Professor Leonard B. Loeb, under whom this study was carried out, for his continued guidance and support, and Professor

W. B. Kunkel, Dr. P. J. MacVicar-Whelan, and Dr. D. A. MacLennan for valuable discussions. Support from the U. S. Office of Naval Research

is gratefully acknowledged, as well as a stipend from the German National Scholarship Foundation for postgraduate studies in the U. S.

*Research supported by the U. S. Office of Naval Research.

†Present address: University of Pittsburgh, Department of Physics, Pennsylvania 15213.

¹M. N. McDermott and W. L. Lichten, *Phys. Rev.* **119**, 134 (1960).

²C. Kenty, *J. Appl. Phys.* **21**, 1309 (1950).

³For a summary of the older data, see H. S. W. Massey and E. H. S. Burhop, *Electronic and Atomic Impact Phenomena* (Clarendon Press, Oxford, 1952).

⁴H. M. Jongerius, W. van Egmund, and J. A. Smit, *Physica* **22**, 845 (1956).

⁵R. J. Anderson, Edward T. P. Lee, and Chun C. Lin, *Phys. Rev.* **157**, 31 (1967).

⁶I. P. Zapesochny and O. B. Shpenik, *Dokl. Akad. Nauk SSSR* **160**, 1053 (1965) [English transl.: *Soviet Phys. - Doklady* **10**, 140, (1965)]; I. P. Zapesochny and O. B. Shpenik, *Zh. Eksperim. i Teor. Fiz.* **50**, 890 (1966) [English transl.: *Soviet Phys. - JETP* **23**, 592, (1966)].

⁷R. W. Rostron, *J. Appl. Phys.* **35**, 2291 (1964).

⁸R. N. Varney, *Phys. Rev.* **157**, 116 (1967).

⁹W. Lichten, *Phys. Rev.* **109**, 1191 (1958).

¹⁰R. E. Fox, W. M. Hickam, D. J. Grove, and T.

Kjeldaas, Jr., *Rev. Sci. Inst.* **26**, 1101, (1955).

¹¹H. D. Hagstrum, *Phys. Rev.* **96**, 336 (1954).

¹²G. J. Schulz, *Phys. Rev.* **112**, 150 (1958).

¹³H. Maier-Leibnitz, *Z. Physik* **95**, 499 (1935).

¹⁴G. J. Schulz and R. E. Fox, *Phys. Rev.* **106**, 1179 (1957).

¹⁵D. A. MacLennan, *Phys. Rev.* **148**, 218 (1966).

¹⁶For details see W. L. Borst, Ph.D. thesis, University of California, Berkeley, 1968 (unpublished).

¹⁷W. M. Hickam, *Phys. Rev.* **95**, 703 (1954).

¹⁸W. B. Nottingham, *Phys. Rev.* **55**, 203 (1939).

¹⁹B. L. Moiseiwitsch and S. J. Smith, *Rev. Mod. Physics* **40**, 238 (1968).

²⁰S. Sonkin, *Phys. Rev.* **43**, 788 (1933).

²¹H. E. Hinteregger and K. Watanabe, *J. Opt. Soc.* **43**, 604 (1953).

²²G. L. Weessler, *Handbuch der Physik*, edited by S. Flügge (Springer-Verlag, Berlin, 1956), Vol. XXI, pp. 304 ff.

²³C. E. Kuyatt, J. A. Simpson, and S. F. Mielczarek, *Phys. Rev.* **138**, A 385 (1965).

²⁴P. D. Burrow, *Phys. Rev.* **158**, 65 (1967).

²⁵H. Beutler, *Z. Physik* **86**, 710 (1933).